

# Simultaneous Optimization of an IGCC Process with Equation-Oriented Methods

Keat Ping Yeoh, Chi Wai Hui\*

Department of Chemical and Biological Engineering, The Hong Kong University of Science and Technology, Clear Water Bay, Kowloon, Hong Kong SAR, China.  
 kehui@ust.hk

Simultaneous optimization of process flowsheets using equation-oriented (EO) methods is a promising alternative to simulation studies. With the use of EO methods, simultaneous optimization of all process units including heat integration can be performed to achieve goals such as maximizing profit or minimizing operating costs. The use of EO methods required the development of new process models and equations of state (EOS), as algorithms and some formulations used in sequential methods do not work in an EO environment. Advancements in EO methods, along with the growth of gradient-based solvers, have enabled large-scale simultaneous flowsheet optimization. However, simultaneous process optimization still faces challenges as large problems, especially non-linear ones, may not achieve convergence without good initial values. A study on the simultaneous optimization of the integrated gasification and combined cycle (IGCC) process using EO methods was conducted as it is a combination of a cryogenic air separation unit (ASU), a coal gasifier and power generation units consisting of a combustor, a gas turbine, a heat recovery steam generator (HRSG) and a steam turbine. The purity of the oxygen product fed to the gasifier was often considered to be fixed in prior IGCC studies. With the ASU model and gasifier model used, the influence of oxygen purity and flowrate fed to the gasifier can be studied. The thermal efficiency of the IGCC process was maximized in GAMS using full-order EO process models. After the optimization, the thermal efficiency increased from 27.7 % in the base case to 36.7 %, with a notable change in process parameters, showing that the solver did not terminate close to the starting solution. Results showed that lowering the oxygen product purity from 95 % to 58.6 % increased the thermal efficiency of the IGCC process as the power required by the compressor in the ASU was reduced.

## 1. Introduction

Increasing the energy efficiency of chemical processes reduces the amount of fossil fuels needed to meet existing power requirements, thus lessening the carbon emissions and pollution associated with power generation. Optimization of these processes to improve performance can be done using sequential modular (SM) methods or EO methods. Many optimization studies are conducted using commercial simulation software such as Aspen Plus, which uses SM methods to solve the process unit models in sequence. However, the success of simulation studies in identifying better process conditions depend on the user's expertise and luck and convergence of complex flowsheets may be difficult to achieve without proper knowledge of the process. For example, process models with recycle streams require many iterations for the solution, leading to difficulties in convergence without good initial values set by the user. EO methods suffer less from these drawbacks, as gradient information can be used to solve the entire process model while simultaneously optimizing an objective function and satisfying constraints. Notably, recycle streams do not increase the difficulty of converging an EO system, as they are treated the same as other streams. While EO methods offer many advantages over SM methods, they are sometimes difficult to implement as process models developed for SM methods are not always applicable to simultaneous optimization using EO methods. EO models also require systematic initialization, but this is no different from SM methods.

Although many ingenious process models have been developed for use with EO methods, simultaneous optimization of large systems using these methods is still not widespread. Instead, optimization is often done by coupling commercially available simulators with external tools such as Excel VBA or MATLAB as the optimizer

(Asprion and Bortz, 2018). Optimization studies using full-order EO models typically have less than 10 free variables, such as the air separation unit (ASU) investigated by Yeoh and Hui (2021) and the ethylene-to-ethanol process used as a motivating example by Pattison and Baldea (2014). Despite the small number of free variables, the resultant system of variables and equations is not small, especially when distillation columns are present. Reduced-order models are sometimes used to decrease the problem size. For example, simultaneous optimization of an IGCC using EO methods has been studied by Wang et al. (2019). However, their work utilized reduced-order models for the ASU and gasifier. While they are useful in reducing the size and complexity of a problem, the usage of reduced-order models and surrogate models may limit the scope of the study as these models may be valid only over a specific operating range. Wang et al. (2019) fixed the purity of oxygen fed to the gasifier at 99 mol%  $O_2$ , but the  $O_2$  purity has a large impact on the power consumption of the ASU. The simplified gasifier model used only considered  $CO$ ,  $CO_2$ ,  $H_2$ ,  $CH_4$  and  $H_2O$  as components in the gasifier outlet and cannot be used to study the effect of oxygen purity on the thermal efficiency of the IGCC process. Equation-oriented simultaneous optimization of complex process flowsheets with more process units and free variables can be used to comprehensively study the interaction between process parameters. In this work, simultaneous optimization of a process with full-order models is presented using a case study on an IGCC, as it contains complex units such as distillation columns and multi-stream heat exchangers (MHEX) in the ASU and a Gibbs free energy minimization reactor used to represent the gasifier. With the gasifier model and full-order ASU model used that includes rigorous material, equilibrium, summation and heat (MESH) equations and pressure drop considerations for the distillation columns and a heat integration model for the MHEX, the effect of oxygen purity and flowrate on the performance of the IGCC can be investigated.

## 2. Process flowsheet and description

The process flowsheet used in the case study is shown in Figure 1. Process constraints are applied based on the ranges in the publication by Wang et al. (2019), though the composition of the oxygen and nitrogen products from the ASU are not fixed at 99 mol%. Air is first separated in the ASU to produce oxygen-enriched air, which is compressed, then fed to the gasifier along with coal and pumped water. Information on the ASU, including the flowsheet and process configuration, can be found in the work by Yeoh and Hui (2021). The gasifier is operated at a pressure between 0.1 – 4 MPa, and the temperature is between 1,100 – 1,600 °C. Syngas from the gasifier enters a heat exchanger to produce steam at 10 MPa and is cooled to 200 °C to before being cleaned in a scrubber to wash off ash and other solid impurities. The clean syngas is then burnt in a combustor between 1.01 and 2.03 MPa with the exit temperature of the hot flue gas being between 1,027 and 1,327 °C. Hot flue gas from the combustor is then expanded to atmospheric pressure in a gas turbine to produce electricity. As the flue gas is still at a high temperature after exiting the turbine, it is used to generate steam in the heat recovery steam generator (HRSG). The pressure and temperature of the generated steam is set to be the same as the steam produced in the syngas cooler. Both steam streams are then expanded to atmospheric pressure in the steam turbine to produce electricity. A condenser cools the steam exiting the turbine to the liquid state. The water stream is then pumped to 10 MPa and recycled as boiler feed water (BFW) to the syngas cooler and HRSG. Although carbon capture is not considered in this study, the key units of the IGCC process are present and the EO model can be readily modified to accommodate carbon capture units when emissions are of particular concern, such as in the study on emergy by Ren et al. (2020). Illinois #6 coal is fed at 10,000 kg  $h^{-1}$  to the gasifier. Sulfur and chlorine are assumed not to be present. The proximate and ultimate analysis provided by Emun et al. (2010) are adjusted to reflect this.

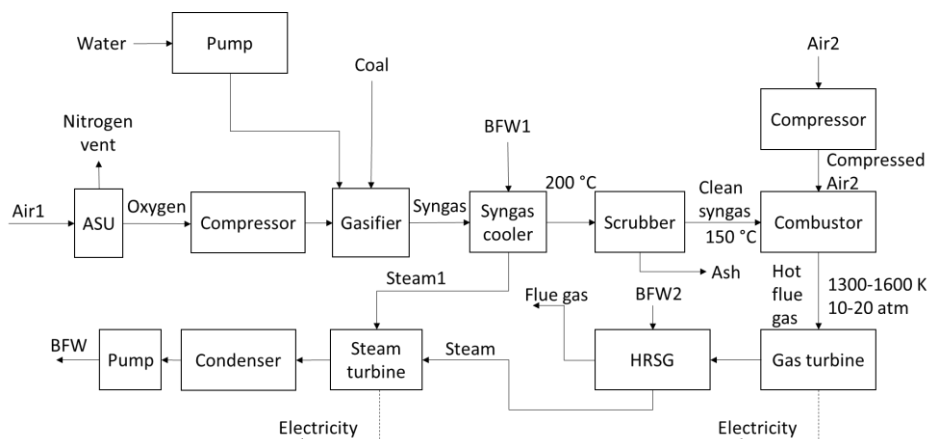


Figure 1: Process flowsheet used in the case study on an IGCC

### 3. Methodology

Mathematical models of various process units are used to represent the IGCC process. The IDEAL method was used as the thermodynamic package to predict stream properties, with the equations and coefficients retrieved from the Help Manual and databank in Aspen Plus V11 (2021). This method was selected as it is the basis of other more complex thermodynamic methods. Process design parameters are optimized based on the process at steady-state and without heat loss to the surroundings. The optimization problem is implemented in GAMS v24.7 and solved as a non-linear programming (NLP) problem using CONOPT. This solver was selected as it is recommended in the GAMS documentation (Drud, 2021) for large nonlinear systems.

#### 3.1 Modeling of the ASU

The distillation columns in the ASU are modeled using the NLP distillation model with grouped bypass efficiencies (Yeoh and Hui, 2021), while the MHEX is modeled with an adapted version of the NLP energy targeting model in Hui (2014), with the utility targets set to 0.

#### 3.2 Gasifier model

The gasifier is modeled using the Gibbs free energy minimization method to predict the composition of the syngas. Kuhn-Tucker conditions are applied to represent the minimization using an equality constraint to avoid a dual objective stemming from concurrently minimizing the Gibbs free energy of the syngas and maximizing the thermal efficiency of the entire system. Enthalpy and element balances are also applied and are represented in Eq(1) and Eq(2), where  $H$  is the enthalpy of the stream,  $f_i$  is the molar flowrate of the component and  $n_{i,el}$  is the number of atoms of an element,  $el$  in the component  $i$ , e.g.  $n_{CO_2,C} = 1$ . Another necessary constraint is that the molar flowrate of each component in the syngas stream must be non-negative, as shown in Eq(3).

$$H^{water} + H^{coal} + H^{oxygen} = H^{syngas} \quad (1)$$

$$E_{el} = f_i^{water} n_{i,el} + f_i^{coal} n_{i,el} + f_i^{oxygen} n_{i,el} - \sum_i f_i^{syngas} n_{i,el} = 0 \quad (2)$$

$$f_i^{syngas} \geq 0 \quad (3)$$

Eq(4) is used to compute  $G_i$ , the molar Gibbs free energy of a component, while the mixture Gibbs free energy of syngas is represented by Eq(5).  $G_i^{form}$  is the Gibbs free energy of formation of a component from its constituent elements at the reference pressure (1 atm) and temperature (25 °C),  $C_i^{P,IG}$  is the ideal gas heat capacity,  $H_i^{form}$  is the enthalpy of formation of component  $i$  and  $y_i$  is the vapor molar fraction of component  $i$ .

$$G_i^{syngas} = G_i^{form} + \int_{T^{ref}}^T C_i^{P,IG} dT - T \int_{T^{ref}}^T \frac{C_i^{P,IG}}{T} dT - \frac{(T - T^{ref})(H_i^{form} - G_i^{form})}{T^{ref}} + RT \ln\left(\frac{P}{P^{ref}}\right) \quad (4)$$

$$G^{syngas} = \sum_i \{f_i [G_i^{syngas} + RT \ln(y_i^{syngas})]\} \quad (5)$$

According to the Karush-Kuhn-Tucker conditions, there is a constant,  $\lambda_{el}$ , for each element balance in Eq(2) as they are equality constraints (Neron et al., 2012). There is also a constant,  $v_i$ , for each component based on the inequality constraint in Eq(3). Consequently, Eq(7) shows the necessary condition for the Gibbs free energy of the system to attain a minimum. Eq(3) is reformulated into the equality constraint in Eq(6), where  $\sigma_i$  is a slack variable that can take on any value. Taking the square of  $\sigma_i$  ensures that  $f_i$  is positive as long as Eq(6) is satisfied. The derivative in Eq(8) is used to relate the value of  $v_i$  to whether the inequality constraints are active.

$$I_i = f_i^{syngas} - \sigma_i^2 = 0 \quad (6)$$

$$\nabla G(f_i) + \sum_{el} \lambda_{el} \nabla E_{el}(f_i) + \sum_i v_i \nabla I_i(f_i) = G_i^{syngas} + RT \ln(y_i^{syngas}) + \sum_{el} (\lambda_{el} n_{i,el}) + v_i = 0 \quad (7)$$

$$v_i \nabla I_i(\sigma_i) = -2v_i \sigma_i = 0 \quad (8)$$

### 3.3 Modeling of the combustor

The combustor where clean syngas is mixed with compressed air to be burnt can be modeled as a stoichiometric reactor where only combustion reactions occur. Only the complete combustion of CO, H<sub>2</sub> and CH<sub>4</sub> are considered as the formation of NO<sub>x</sub> has a high activation energy and it is assumed that no sulfur is present in the system. A constraint of at least 3 mol% of O<sub>2</sub> in the combustor outlet is enforced to ensure complete combustion. Enthalpy balance is also applied. The representative equations are shown in Eq(9) and Eq(10).

$$f_i^{Hot\ flue\ gas} = f_i^{clean\ syngas} + f_i^{Compressed\ Air2} + Generation - Consumption \quad (9)$$

$$H^{Clean\ syngas} + H^{Compressed\ air} = H^{Hot\ flue\ gas} \quad (10)$$

### 3.4 Models for the syngas cooler, HRSG and scrubber

The syngas cooler and HRSG are modeled as countercurrent heat exchangers. There is no composition change of the hot and cold streams. A minimum temperature approach,  $\Delta T^{min}$  of 10 °C is enforced at both ends of the heat exchanger to ensure feasible heat transfer, as shown in Eq(11) and (12). Eq(13) shows the enthalpy balance. The value of  $\Delta T^{min}$  was selected based on design heuristics to balance the tradeoff between capital and operating costs since the area of the heat exchanger is not calculated explicitly. It is assumed that there is no pressure drop across the heat exchanger since the detailed design is not available in the conceptual stage.

$$T^{Hot\ stream\ in} - T^{Cold\ stream\ out} \geq 10\ ^\circ C \quad (11)$$

$$T^{Hot\ stream\ out} - T^{Cold\ stream\ in} \geq 10\ ^\circ C \quad (12)$$

$$H^{Hot\ stream\ in} - H^{Hot\ stream\ out} = H^{Cold\ stream\ out} - H^{Cold\ stream\ in} \quad (13)$$

Ash and other impurities are washed out in the scrubber. It is assumed that none of the water used in the scrubbing vaporizes into the syngas and all of the ash is removed. A temperature drop of 50 °C is applied here.

### 3.5 Modeling of pumps, compressors and expanders

As the pumps are only used to raise the pressure of liquid water, it is assumed that the fluid is incompressible. The work done by the pump is calculated by Eq(14), assuming an isentropic efficiency,  $\eta^{isen}$ , of 30 %. Work done by the compressors and expanders is calculated with the isentropic using GPSA method shown in Eq(15). The temperature and heat capacity ratios are assumed to be the same as that of the inlet.

$$work^{pump} = \frac{f_{H_2O}^{water} \bar{V}^l (P^{out} - P^{in})}{\eta^{isen}} \quad (14)$$

$$work^{comp/exp} = \frac{\frac{f^{inlet} RT}{(\frac{\gamma-1}{\gamma})} \left[ \left( \frac{P^{out}}{P^{in}} \right)^{\frac{\gamma-1}{\gamma}} - 1 \right]}{\eta^{comp,isen}} \eta^{exp,isen} \quad (15)$$

$$\gamma = \frac{C^p}{C^v} = \frac{C^p}{C^p - R} \quad (16)$$

$$H^{out} = H^{in} + work \quad (17)$$

$\bar{V}^l$  is the liquid molar volume and  $\gamma$  is the ratio of the constant pressure heat capacity to the constant volume heat capacity. The default value in Aspen Plus of  $\eta^{isen} = 72\%$  is used for the compressors and expanders. Energy balance equations shown in Eq(17) are also applicable to these equipment.

### 3.6 Thermodynamic modules and the objective function

$C_i^{P,IG}$  is calculated as shown below in Eq(18), where the coefficients  $A_i^I$  to  $A_i^V$  are obtained from Aspen Plus (2021). Eq(19) is used to calculate the enthalpy.  $\Delta H_i^{vap}$  is the heat of vaporization of component  $i$  and the parameters  $B_i^I$  to  $B_i^V$  shown in Eq(20) were also extracted from Aspen Plus (2021).

$$C_i^{P,IG} = A_i^I + A_i^{II} \left[ \frac{A_i^{III}}{T \text{SINH} \left( \frac{A_i^{III}}{T} \right)} \right]^2 + A_i^{IV} \left[ \frac{A_i^V}{T \text{COSH} \left( \frac{A_i^V}{T} \right)} \right]^2 \quad (18)$$

$$H = \sum_i \left[ f_i^{vap} \left( \int_{T^{ref}}^T C_i^{P,IG} dT + H_i^{form} \right) \right] + \sum_i \left[ f_i^{liq} \left( \int_{T^{ref}}^T C_i^{P,IG} dT - H_i^{vap} + H_i^{form} \right) \right] \quad (19)$$

$$\Delta H_i^{vap} = B_i^I \left( 1 - \frac{T}{T^c} \right)^{B_i^{II} + \frac{B_i^{III} T}{T^c} + B_i^{IV} \left( \frac{T}{T^c} \right)^2} \quad (20)$$

The enthalpy of coal can be estimated using Eq(21) and the correlation for the mass enthalpy of ash is fitted from Aspen Plus using a quadratic equation shown in Eq(22), where T is in °C. Only the products from the complete combustion of coal with regard to the ultimate analysis are considered in Eq(21).

$$H^{coal} = LHV_{coal} + \sum_{i \in COMB} f_i H_i^{form} \quad (21)$$

$$H^{Ash} = 2.9299 \times 10^{-4} T^2 + 0.7538 T - 822.7537 \quad (22)$$

The objective function maximized in the optimization study in GAMS is the thermal efficiency in Eq(23).

$$Obj = \eta^{thermal} = \frac{\sum \text{Net work of compressors, pumps and expanders}}{LHV} \times 100 \% \quad (23)$$

#### 4. Results and discussion

A base case was obtained using the GAMS model with process parameters fixed or allowed to vary within a narrow range. The base case obtained from GAMS was simulated in Aspen Plus to ensure that there were no mistakes in the implementation of the GAMS model and there were no discrepancies. With the base case as an initial starting point, the previously fixed process parameters were relaxed and the optimization was conducted. The thermal efficiency of the optimized case is similar to that found by Emun et al. (2010) in their simulation study, but lower than the one reported by Wang et al. (2019). The difference may be due to the different isentropic efficiencies used and the simplifications made to the process models by Wang et al. (2019).

A comparison between the base case and the final optimized solution shown in Table 1 demonstrated a significant improvement in the objective value and notable differences in the optimized process parameters.

Table 1: Comparison between the base case and the optimized case

	Base case	Optimized case
Thermal efficiency/%	27.72	36.69
Net work produced/MW	19.95	26.41
Net work consumed in the ASU/MW	1.96	0.47
Oxygen product purity/%	95.00	58.60
Oxygen stream flowrate/kmol h <sup>-1</sup>	243.46	142.95
Total number of distillation stages in the ASU	18	8
Top stage pressure of the high pressure column in the ASU/MPa	0.41	0.21
Water fed to the gasifier/kmol h <sup>-1</sup>	250.00	36.54
Gasifier temperature/°C	1,205.01	1,100.00
Gasifier pressure/MPa	3.00	1.01
Work consumed to compress combustion air/MW	30.01	20.86
Combustion temperature/°C	1,326.85	1,326.85
Combustion pressure/MPa	2.03	1.01
Work produced in the gas turbine/MW	42.78	34.28
Work produced in the steam turbine/MW	10.99	14.53
Total steam produced/kmol h <sup>-1</sup>	3,167.24	2,570.06
Temperature of steam produced/°C	449.02	846.35

The thermal efficiency increased to 36.7 %, exhibiting a 32 % improvement relative to the base efficiency of 27.7 %, showing that the model did not get stuck at neighborhood solutions close to the initial point during the optimization procedure. One of the major reasons for the improvement is the decrease in oxygen purity and flowrate fed to the gasifier, which reduced the power consumed in the ASU by 76 %. The number of stages in the distillation columns also decreased due to the lower purity requirement, which would reduce the capital cost. This is an encouraging result that shows the success in optimizing a large and complex process flowsheet using EO methods. For comparison, the IGCC model is much larger than the ASU model in the case study by Yeoh and Hui (2021), where the IGCC model has 4,447 equations and 4,434 variables compared to 2,933 equations and 2,513 variables in the ASU model. The solution speed is also fast with the IGCC model being solved in a mere 14 s, about double of the time taken to solve the ASU model.

## 5. Conclusions and future work

Optimization of a complex and large-scale process flowsheet using full-order EO models was conducted using GAMS with a case study on an IGCC. In particular, the study served to study the effect of oxygen purity and flowrate on the thermal efficiency. It was observed that reducing the oxygen purity to 58.6 % was optimal due to significant energy savings of 76 % in the ASU. Despite the complexity of the unit operation models and the size of the resultant EO model, the objective value showed an improvement of 32 % relative to the initial case. The free variables also exhibited large differences compared the base case, showing that the solution did not remain close to the initial value even for a highly non-linear system. Furthermore, the solution was obtained in less than half a minute, which is encouraging as this means that even larger systems could be solved within a reasonable duration. The results of the case study show that optimization of full-order complex flowsheets with EO methods yields meaningful results. However, more work should be done to improve the approach taken. For example, thermodynamic modules such as cubic equations-of-state (EOS) could be used in the future to represent the physical properties more accurately as they account for interactions between the components. They can be selected based on EOS models used for simulations in the industry and academia. These cubic EOS models are an extension to the IDEAL method used in this work, as properties such as the ideal gas enthalpy and Gibbs free energy remain in use. The cubic EOS models merely add departure terms to certain IDEAL method values. Other than that, multi-start methods could be considered to find a better optimum value.

## Acknowledgements

The authors are appreciative of the financial support provided by the Hong Kong Research Grants Council General Research Fund (RGC-GRF 16211117).

## References

- Aspen Plus V11, 2019, USA: Aspen Technology, Inc. <[www.aspentech.com/en/products/engineering/aspen-plus](http://www.aspentech.com/en/products/engineering/aspen-plus)>, accessed 21.05.2021.
- Asprion N., Bortz M., 2018, Process modeling, simulation and optimization: from single solutions to a multitude of solutions to support decision making, *Chemie Ingenieur Technik*, 90(11), 1727-1738.
- Drud A., 2021, CONOPT, ARKI Consulting and Development A/S, Bagsvaerd, Denmark. [www.gams.com/latest/docs/S\\_CONOPT.html](http://www.gams.com/latest/docs/S_CONOPT.html), accessed 10.06.2021.
- Emun F., Gadalla M., Majozi T., Boer D., 2010, Integrated gasification combined cycle (IGCC) process simulation and optimization, *Computers & Chemical Engineering*, 34(3), 331-338.
- Hui C.W., 2014, Optimization of heat integration with variable stream data and non-linear process constraints, *Computers & Chemical Engineering*, 65, 81-88.
- Néron A., Lantagne G., Marcos B., 2012, Computation of complex and constrained equilibria by minimization of the Gibbs free energy, *Chemical Engineering Science*, 82, 260-271.
- Pattison R. C., Baldea M., 2014, Equation-oriented flowsheet simulation and optimization using pseudo-transient models, *AIChE Journal*, 60(12), 4104-4123.
- Ren S., Feng X., Wang Y., 2020, Energy Evaluation of IGCC Power Generation with a Carbon Capture System, *Chemical Engineering Transactions*, 81, 37-42 DOI:10.3303/CET2081007
- Wang M., Liu Q., Liang Y., Hui C. W., Liu G., 2019, Reduced Integration Optimization Model for Coupled Elevated-Pressure Air Separation Unit and Gas Turbine in Oxy-combustion and Gasification Power Plant. *Process Integration and Optimization for Sustainability*, 3(1), 143-156.
- Yeoh K. P., Hui C. W., 2021, Rigorous NLP distillation models for simultaneous optimization to reduce utility and capital costs, *Cleaner Engineering and Technology*, 2, doi.org/10.1016/j.clet.2021.100066